Biochimica et Biophysica Acta 1798 (2010) 21–31

Contents lists available at ScienceDirect

Biochimica et Biophysica Acta

journal homepage: www.elsevier.com/locate/bbamem

The influence of different membrane components on the electrical stability of bilayer lipid membranes

Iris van Uitert, Séverine Le Gac, Albert van den Berg *

BIOS the Lab-on-a-Chip group, MESA+ Institute for Nanotechnnology, University of Twente, Postbus 217, 7500 AE Enschede, The Netherlands

ARTICLE INFO

Article history:
Received 9 April 2009
Received in revised form 1 October 2009
Accepted 6 October 2009
Available online 14 October 2009

Keywords:
Electroporation
BLM
Cell membrane
Pore formation
(Phospho)lipid
Channel protein

ABSTRACT

A good understanding of cell membrane properties is crucial for better controlled and reproducible experiments, particularly for cell electroporation where the mechanism of pore formation is not fully elucidated. In this article we study the influence on that process of several constituents found in natural membranes using bilayer lipid membranes. This is achieved by measuring the electroporation threshold (V_{th}) defined as the potential at which pores appear in the membrane. We start from highly stable 1,2-diphytanoyl-*sn*-glycero-3-phosphocholine (DPhPC) membranes (V_{th} ~200 mV), and subsequently add therein other phospholipids, cholesterol and a channel protein. While the phospholipid composition has a slight effect (100 mV$\leq V_{th} \leq$290 mV), cholesterol gives a concentration-dependent effect: a slight stabilization until 5% weight (V_{th} ~250 mV) followed by a noticeable destabilization (V_{th} ~100 mV at 20%). Interestingly, the presence of a model protein, α-hemolysin, dramatically disfavours membrane poration and V_{th} shows a 4-fold increase (~800 mV) from a protein density in the membrane of 24×10^{-3} proteins/μm^2. In general, we find that pore formation is affected by the molecular organization (packing and ordering) in the membrane and by its thickness. We correlate the resulting changes in molecular interactions to theories on pore formation.

1. Introduction

A cell membrane consists of a (phospho)lipid matrix defining its structure and shape and serving as a substrate for membrane proteins. Phospholipids are composed of two main parts: (i) a hydrophilic head consisting of a backbone molecule (either glycerol or sphingosine), a phosphate and a polar group and (ii) two "parallel" hydrophobic chains (saturated or unsaturated and of various lengths). Due to their amphiphilic structure, phospholipid molecules self-assemble into micelle or bilayer structures when placed in aqueous solutions. The properties of phospholipids are determined by the length of the hydrocarbon chains, the amount of unsaturations present in the chains, the molecular shape and the nature of the head group. These distinct properties of phospholipids affect their packing density and consequently the fluidity and stability of the membranes. Another important lipidic constituent of the cell membrane is cholesterol that typically represents 30% mole of the lipid matrix. Cholesterol greatly affects the fluidity of the membrane by establishing specific interactions with the hydrocarbon chains and head groups of the phospholipids [1]. The last main component found in cell membranes is proteins which account for 50% of the membrane weight [2]. The so-called transmembrane proteins span the membrane and present hydrophilic parts eventually protruding on both sides and a hydrophobic part located in the hydrophobic core of the membrane.

A cell membrane forms an impermeable barrier to foreign entities, among which genes, drugs, particles, and certain dyes. For many applications, such as DNA transfection or drug research, it is necessary to transport these substances into a cell, and this requires the transient permeabilization of the cell membrane. A commonly used technique for this purpose is electroporation [3-5]. Thereby, pores are temporarily created in the membrane upon application of a high external electric field (kV/cm), usually short DC pulses (μs–ms range) or exponentially decaying pulses [6]. When the imposed transmembrane potential reaches a threshold value of about 0.2–1 V, a rearrangement in the molecular structure of the membrane occurs, leading to the formation of pores and a substantial increase in the cell's permeability to ions and molecules. These last few decades, the popularity of the technique of electroporation has been increasing, notably for cell transfection [7,8]. However, the overall success rate of the process remains low: using batch electroporation typically only 40% to 70% of the cells are viably electroporated [9], most of them remain viable while being unaffected by the electrical stimulus and a small amount dies. Indeed, the whole process is difficult to control at

Abbreviations: DPhPC, 1,2-Diphytanoyl-*sn*-glycero-3-phosphocholine; PS, Porcine brain l-α-phosphatidylserine; PI, Bovine liver l-α-phosphatidylinositol; PE, Bovine heart l-α-phosphatidylethanolamine; PC, Phosphatidylcholine; Ch, Cholesterol; BLM, Bilayer lipid membrane; V_{th}, Electroporation threshold voltage

* Corresponding author. Tel.: +31 53 489 2724; fax: +31 53 489 3595.
E-mail address: a.vandenberg@utwente.nl (A. van den Berg).

0005-2736/$ – see front matter © 2009 Elsevier B.V. All rights reserved.
doi:10.1016/j.bbamem.2009.10.003

the level of a cell population as the outcome of the electroporation process depends on a number of uncontrollable parameters, such as the cell size, shape and "vulnerability" [6].

One approach to increase the success rate of electroporation experiments, consists of getting a better understanding of the mechanism(s) of pore formation and identifying key-parameters for this process through experimental work and/or theoretical modelling. Studies on the mechanism of pore formation provide insight into the pore location and into the sequence of molecular events leading to pore formation. For instance, the comparison between the electrical breakdown of cell membranes and lipid membranes has demonstrated that the pores originate in the lipid matrix of the membrane [10]. Furthermore, molecular dynamics simulations have demonstrated that the formation of a pore proceeds in three steps upon application of a potential across the membrane. In the first stage, the electric field is locally enhanced, causing water defects in the bilayer structure. In the second stage, water molecules form a water file that spans the bilayer by establishing hydrogen bonds with each other. In the last stage, molecular rearrangement of the phospholipids in the vicinity of this water defect occurs and phospholipid molecules move towards this water channel to give a hydrophilic pore lined with phospholipid head groups [11,12]. Pores start to form nano- to microseconds after application of the electric field [12-15], expand in a few milliseconds and close again in seconds to minutes in cells and milliseconds to seconds in artificial membranes [10,14,16,17]. The diameter of an electropore varies from 0.5 to 400 nm [12,13,15,18].

Another crucial aspect towards understanding the process of electroporation is the identification of key parameters affecting the stability of membranes. Experimental and theoretical studies have shown that this strongly depends on the composition of the membrane: the structural properties of the phospholipids found therein and the presence and amount of other membrane constituents. For instance, the electroporation threshold depends on the bilayer thickness, and consequently on the length of the phospholipid hydrocarbon chains [19,20]. Another key-factor is the presence of non-zero intrinsic monolayer curvature phospholipids in the membrane. Such lipids have a conical shape with either a large head group (positive intrinsic monolayer curvature) or a small head group (negative intrinsic monolayer curvature) compared to the hydrocarbon chains. These molecules cause packing defects in the membrane that facilitate the process of pore formation [21,22]. Interestingly, it has been demonstrated that the head group charge does not influence the membrane stability although one could expect that electrostatic interactions (repulsion or attraction) between different head groups would result in a change in the packing density of the membrane [19,20]. A second membrane compound of importance is cholesterol; it affects membrane properties not only through specific interactions with the hydrocarbon chains [23-27] but also because of its negative intrinsic monolayer curvature [21,28-30]. Depending on the nature of the phospholipid molecules and the amount of cholesterol used this effect can be two-fold [24,31-33]. The last main component found in natural membranes, peptides and proteins, also influences the stability although this phenomenon is still poorly understood. For instance, Troiano et al. [34] showed that the presence of small peptides such as gramicidin A and D in the membrane decreases the probability of pore formation. Recent molecular dynamics studies have corroborated these results [35,36].

Alternatively, external (natural or synthetic) molecules can also be employed to modulate the membrane properties: they strengthen molecular interactions between phospholipids or loosen the intermolecular structure of the membrane. For instance, both the detergent octaethyleneglycol mono n-dodecyl ether ($C_{12}E_8$) [37] and the solvent dimethylsulfoxide (DMSO) [38] decrease the stability of the membranes by acting as a positive curvature molecule. Additionally, the surfactant sodium dodecyl sulfate (SDS) reduces the membrane stability by lowering the interactions between phospholipid molecules due to its incorporation in the cell membranes [39]. On the other hand, the addition of the surfactant poloxamer 188 leads to an increase in the membrane stability; this is caused by either specific interactions with the phospholipids or by the formation of an insulating layer at the membrane surface, behaving as a shunting layer for the applied potential [40].

These different results suggest that the molecular aspects of the composition of the membrane are important for the creation of pores and the electrical stability of the membranes, and that the interactions between the different molecules in the membrane are key-parameters in the process of pore formation.

In this article, we aim to get a better insight into the mechanism of electropore formation. For that purpose, we investigate the influence of the membrane composition and of its individual constituents on its (electrical) stability. Our approach consists of using artificial membrane models, bilayer lipid membranes (BLMs) and assessing the membrane stability by measuring the electroporation threshold. This threshold is defined as the potential at which pores are observed in the membrane. The basic "building block" we use to prepare the membranes is a synthetic phospholipid, 1,2-diphytanoyl-*sn*-glycero-3-phosphocholine (DPhPC). This phospholipid is composed of two identical saturated hydrocarbon chains functionalized with methyl groups and a relatively large head group. It yields densely packed and very stable membranes. In a first stage, we investigate to which extent the electrical stability may be affected by the properties of the individual phospholipids present in the membrane. For that purpose, BLMs are prepared using a mixture of two phospholipids; DPhPC mixed with other phospholipids found in natural cell membranes that are unsaturated and have a non-zero intrinsic monolayer curvature. Following this, we examine how cholesterol affects pore formation in DPhPC membranes, and finally the contribution of one type of channel proteins, α-hemolysin, on the same process.

2. Materials and methods

2.1. Chemicals

Lipids (1,2-diphytanoyl-*sn*-glycero-3-phosphocholine (DPhPC), bovine heart l-α-phosphatidylethanolamine (PE), bovine liver l-α-phosphatidylinositol (PI), porcine brain l-α-phosphatidylserine (PS) and cholesterol (Ch) (Fig. 1)) are purchased at Avanti Polar Lipids (Alabaster, AL). The protein α-hemolysin is purchased at Sigma-Aldrich (St. Louis, MO). KCl, Hepes, Tris and n-decane are purchased at Sigma-Aldrich (St. Louis, MO). Chloroform is purchased at Merck Chemicals (Darmstadt, Germany). Deionized water (18.2 mΩ×cm) which is used for all solution preparation and cleaning procedure is obtained using a MilliQ system (Millipore, Billerica, MA).

2.2. Measurement set-up

A conventional bilayer system (Warner Instruments, Hamden, CT) is used for BLM experimentation. This system comprises of a delrin cup and chamber containing two round compartments. The cup is inserted in the *trans*-compartment of the chamber, and the compartments are connected via a 150 μm aperture in the cup across which BLMs are prepared. Both compartments contain 1 mL buffer solution and Ag/AgCl electrodes (used for the electrical characterization of the BLMs). Electrical measurements are carried out with an Axopatch 200b patch-clamp amplifier (Molecular devices, Sunnyvale, CA), applying voltages and measuring currents across the bilayer. Data-acquisition is performed with LabVIEW and a PCI-6259 data acquisition card (National Instruments, Austin, TX).

2.3. Preparation and characterization of BLMs

All lipids are used as chloroform-based solutions. DPhPC and PI are purchased at 10 mg/mL solutions in chloroform. Other lipids (PS, PI,

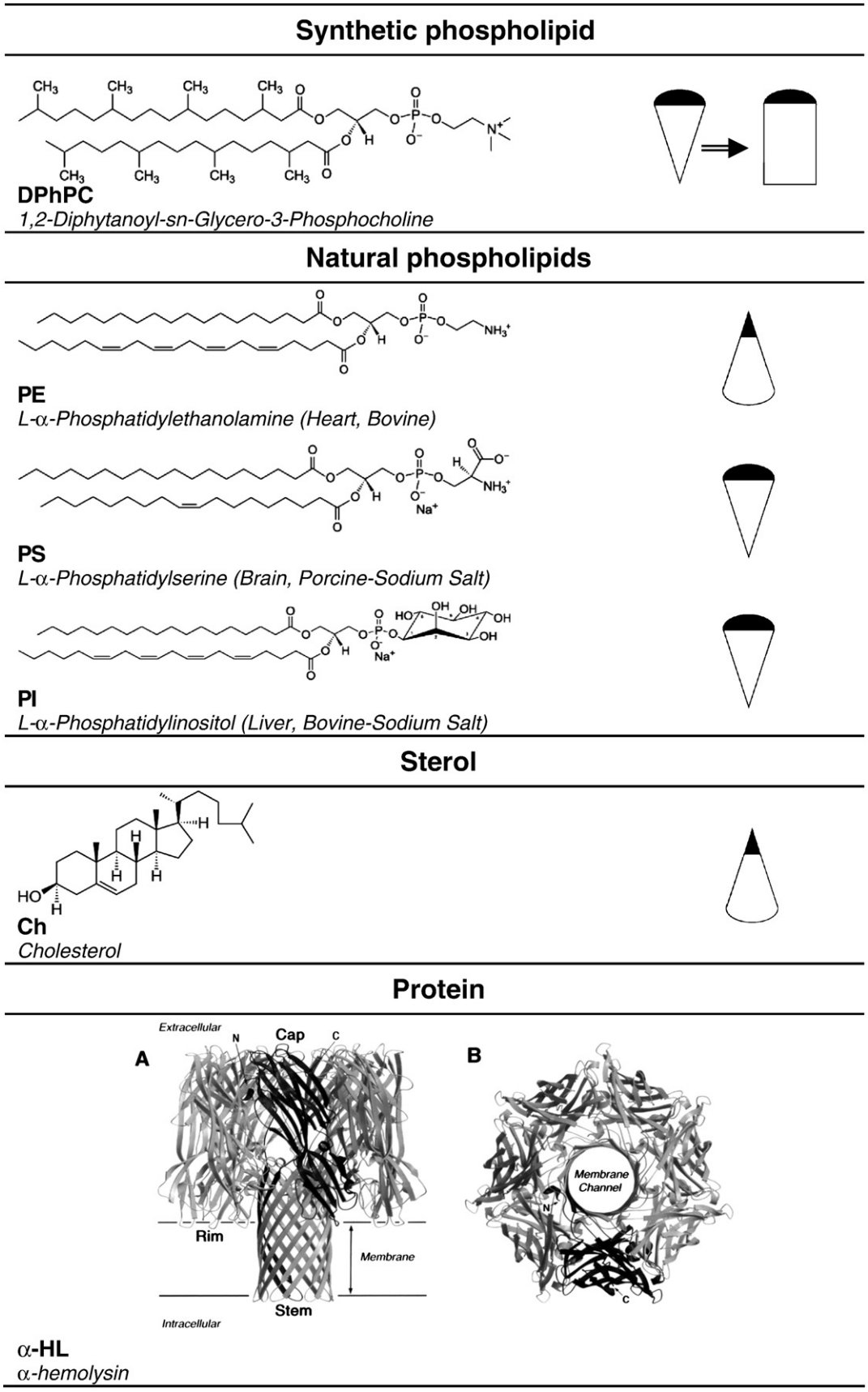

Fig. 1. Molecular structures of the phospholipids used in this study, cholesterol and the protein α-hemolysin [55]. * Reprinted from Journal of structural biology, 121, E. Gouaux, α-Hemolysin from Staphylococcus aureus: An Archetype of β-Barrel, Channel-Forming Toxins, 110-122, Copyright (1998), with permission from Elsevier. In the right column, the corresponding molecular shapes of the phospholipids and cholesterol are shown according to the classification of Israelachvili [29]. DPhPC can have two conformational shapes as explained in more detail in the text.

PE, and Ch) are purchased as powders and dissolved in chloroform to yield 25 mg/mL solutions. Before the preparation of BLMs, a few tenths of μL of the lipid solution in chloroform is left to evaporate overnight, yielding an amount of 500 μg dried lipids, and subsequently dissolved in n-decane at a final concentration of 25 mg/mL. To improve the solubility of the lipids 2–3% ethanol can be added. The resulting n-decane solutions are used for the preparation of BLMs, and eventually mixed with other lipid solutions in case of multi-lipid membranes.

Two buffers are used for the BLM experimentations: a BLM buffer (10 mM Tris, 1 M KCl, pH 8.5) for most experimentations and an α-HL buffer (5 mM Hepes, 1 M KCl, pH 7.4) for experiments with α-hemolysin as using the buffer of pH 8.5 result in a noisy signal when α-hemolysin molecules insert.

Bilayer lipid membranes are created using the Mueller–Rudin technique [41]. Bilayer formation is monitored using the Axopatch amplifier and characterized by a drop in the current due to the GΩ seal between the bilayer and the aperture. Thereafter, the membrane capacitance is measured as previously described [42] to confirm the formation of a BLM and as indication of the membrane properties; the membrane surface area is derived from the capacitance using equation 1:

$$A\left[cm^2\right] = \frac{C_{measured}[\mu F]}{C_{specific}\left[\mu F / cm^2\right]} \quad (1)$$

where A stands for the membrane surface area in cm^2, C_{meas} for the measured capacitance in μF and $C_{specific} = 0.45 \pm 0.05$ μF/cm^2 [43].

2.4. Insertion of protein channels in BLMs

Alpha-hemolysin is dissolved in MilliQ water at a concentration of 2 mg/mL. This initial solution is further diluted before any experiment to the desired concentration. 5 μL of a diluted α-hemolysin solution is added to 1 mL of the buffer (α-HL buffer) in the *cis*-compartment while stirring to promote protein diffusion to the membrane and their insertion. The insertion of individual proteins is monitored by recording the current. Every insertion gives rise to a characteristic jump in the current. After the insertion of a first protein, stirring is stopped as proteins continue inserting in the membrane.

2.5. Determination of the electroporation threshold of BLMs

The electroporation threshold (V_{th}) of the membrane is defined as the voltage at which the membrane conductivity increases due to the creation of pore(s). This value is determined as the value at which a leakage current is measured through the membrane. For that purpose, a DC voltage of 100 mV is applied to the membrane using the Axopatch amplifier and gradually increased (every 30 s) by steps of 20 mV, until peaks larger than three times the root mean-square of the noise are observed in the measured current. Pore formation is checked by re-applying the potential at which peaks are detected; this confirms that the peaks are not due to imperfections in the membrane. The voltage value found corresponds to the electroporation threshold V_{th}. For every membrane composition, V_{th} is determined at least 3 independent times and the indicated value corresponds to the average of the three separate measurements.

3. Results

The ultimate goal of this study is to get a better insight into the influence of the molecular properties and the composition of the cell membrane on the mechanism of (electro)pore formation. For that purpose, we consider phospholipids, cholesterol and proteins found in natural cell membranes. The two main sections of this article focus on the lipidic formulation (phospholipid and cholesterol) and the protein content of the membrane.

3.1. Lipidic structure of membranes

3.1.1. Phospholipid-phospholipid interactions

In the first series of experiments we examine the interactions between different phospholipids placed in a membrane and their influence on the membrane's resistance to an applied electric field. We use membranes prepared from a mixture of two phospholipids, DPhPC and another phospholipid found in cell membranes (DPhPC-PE, DPhPC-PS, and DPhPC-PI), introduced in various weight percentages. We measure the membrane electroporation threshold (V_{th}) of the resulting membranes. Fig. 2A–C illustrates the variations of the measured electroporation threshold V_{th} when the membrane composition is varied from 100% DPhPC membranes to 100% of the second phospholipid.

Some trends are apparent in these variations depending on the added phospholipid molecule. The differences in the membrane stability can be explained by a change in the packing density of the phospholipid molecules. These are induced by the unsaturations present in the hydrocarbon chains of the phospholipids or by their non-zero intrinsic monolayer curvature. Firstly, phospholipids that contain unsaturations in the chain are forced further apart due to kinking of the hydrocarbon chains [2]. Secondly, according to the classification proposed by Israelachvili [29], the packing density of phospholipids correlates with their shape: cylindrical, tapered or frayed (see Fig. 1). The two latter groups display a non-zero intrinsic monolayer curvature (negative or positive, respectively) and the individual molecules prefer to assemble as micellar structures. As a consequence, their presence in a planar membrane results in defects in the molecule packing [21, 38], a decrease in the membrane stability upon application of an external voltage and a facilitated pore formation. These two factors (the eventual presence of unsaturations and the intrinsic monolayer curvature of the phospholipid molecules) correspond well to the observed trends in V_{th} for the three systems considered here.

DPhPC possesses two identical saturated hydrocarbon chains functionalized with four methyl groups (in positions 3, 7, 11 and 15) and a relatively large head group (see Fig. 1). DPhPC molecules are slightly tapered, but once they are introduced in a planar membrane they tend to adopt a cylindrical shape by the formation of interdigitated structures by the methyl-functionalized chains [29,44,45]. As a consequence, the lateral and rotational motion of individual phospholipid molecules is dramatically decreased compared to other PC species [46]. DPhPC forms highly packed and ordered membranes, reflected by their low surface tension (32–37 mN/m vs. 54–56 mN/m for most of the phospholipids) [47] and they are in the liquid crystal phase (between −120°C and 120°C typically). The addition of other (phospho)lipid species in the membrane breaks the DPhPC interdigitated network, allowing molecules to move freely and subsequently yielding less stable membranes.

PE (l-α-phosphatidylethanolamine) was first added in DPhPC membranes. As shown in Fig. 2A, we find a linear decrease in the electroporation threshold upon the progressive introduction of PE in DPhPC membranes: from 204 ± 16 mV for 100% DPhPC membranes to 160 ± 28 mV for 100% PE membranes. This marked decrease in V_{th} is accounted for by both the structural properties of PE molecules and the destruction of the DPhPC intertwined network. The predominant species of the used PE holds four unsaturations (see Fig. 1) so its addition leads to a progressive loosening of the phospholipid packing [2]. Moreover, PE presents a slight conical shape due to its smaller head group where methyl groups are replaced by hydrogen atoms (see Fig. 1). It displays a negative intrinsic monolayer curvature [21,29] and is a non-bilayer preferring lipid under physiological conditions [48]. As a result, PE-based membranes are reported as highly porous [49] with a large amount of packing defects [21]. We can conclude that the linear decrease we see in the electroporation

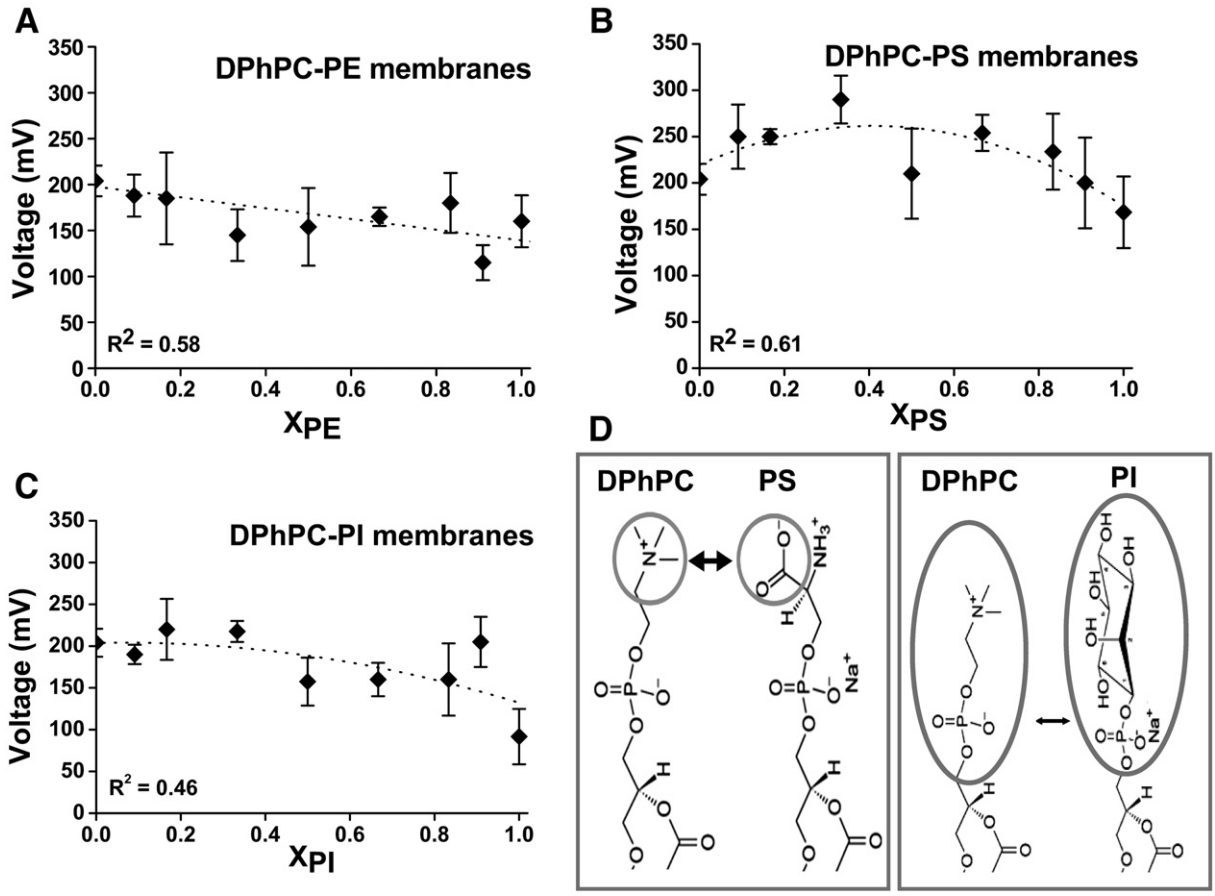

Fig. 2. (A–C) Electroporation threshold V_{th} measured for bi-phospholipid BLMs plotted as a function of the weight percentage of the second phospholipid ($X_{PL} = \frac{M_{PL}}{M_{PL} + M_{DPhPC}}$ where M_{PL} is the amount of phospholipid (PL) (μg) and M_{DPhPC} the amount of DPhPC (μg)). The BLMs are prepared using mixtures of DPhPC-PE (A), DPhPC-PS (B) and DPhPC-PI (C). Dotted lines represent the best fit for the data derived in Origin (OriginLab, Northampton, MA). (D) Illustration of the charge interactions taking place between the negative head groups of PS (left) and PI (right) and the zwitterionic head group of DPhPC.

threshold is caused by the sum of three factors: the loss of the intertwining network, the progressive addition of unsaturations and the introduction of packing defects in the membrane [21,48,49].

A similar trend in the variations of V_{th} was expected for DPhPC-PS systems as the predominant species of the used PS presents one unsaturation, a large head group and consequently a positive intrinsic monolayer curvature. Interestingly, although we measure a lower electroporation threshold for 100% PS membranes (168 ± 39 mV against 204 ± 16 mV for 100% DPhPC membranes), the variations of V_{th} do not follow a monotonous trend upon addition of PS. They resemble the shape of a bell (see Fig. 2B), and V_{th} reaches the maximum value of 290 ± 26 mV around 2:1 DPhPC:PS membranes. Firstly, as for PE, the addition of PS results in a decrease of the phospholipid packing density due to the loss of the chain entanglement and the addition of unsaturations. Furthermore, packing defects are created in the membrane since PS has a positive intrinsic monolayer curvature. However, for low amounts of PS, another phenomenon must counteract these three factors to explain the increase in V_{th} we observe for PS amounts up to around 33%. We attribute this stabilization parameter to electrostatic interactions taking place between the negative charge found in the head group of PS and the zwitterionic head group of DPhPC, as illustrated in Fig. 2D. While it is known from literature that the phospholipid charge does not affect the membrane stability and the process of pore formation [19,20], we hypothesize that this charge interaction strengthens the membrane. As a summary, four contributions are found for DPhPC-PS systems; the same three destabilizing effects as for DPhPC-PE membranes and a counteracting electrostatic stabilizing effect, resulting in the observed bell-shaped variation of V_{th}.

Comparable behaviour is demonstrated for PI (l-α-phosphatidylinositol) which correlates well to the facts that the predominant species of the used PI and PS both present unsaturations (four in the case of PI), a positive intrinsic monolayer curvature and a negative charge (see Fig. 1). As shown in Fig. 2C, V_{th} first remains more or less stable (up to ~33% PI), and subsequently strongly decreases to reach a value of 92 ± 33 mV for mono-PI membranes. This value is notably smaller than the V_{th} observed for 100% PE and PS membranes. The same four contributions are found for PI and PS: three destabilizing contributions (destruction of the DPhPC network, addition of unsaturations and a positive intrinsic monolayer curvature) and one stabilizing contribution (charge interactions between PI and DPhPC head groups (see Fig. 2D)). However, this last stabilizing contribution is quickly overcome by the other opposite factors, most probably due to the higher number of unsaturations found in PI and the larger head group. This translates into the observed plateau in V_{th} for PI amounts lower than ~33%, instead of an increase.

These three series of experiments confirm that the chemical and structural properties of individual phospholipids influence the membrane stability and the creation of pores upon application of an electric field. Depending on the molecular properties of the phospholipids this effect can be either stabilizing or destabilizing. These results also confirm that more than one type of interactions is interfering with this process.

3.1.2. Phospholipid–cholesterol interactions

Another lipidic parameter we consider here is cholesterol, found in natural membranes at up to 14% weight (equivalent to 30% mol) [1,50]. The variations of the electroporation threshold V_{th} for

membranes containing 0–20% weight cholesterol clearly present two different trends (see Fig. 3). At low cholesterol concentrations (1–5%), we observe a progressive increase in V_{th} that reaches the value of 254 ± 13 mV for 5% weight cholesterol. At higher cholesterol concentrations, the tendency is inversed, and the addition of cholesterol leads to a decrease in V_{th} down to 104 ± 52 mV for 20% cholesterol. Interestingly, this final value of V_{th} is approximately half of the value measured for 100% DPhPC membranes (204 ± 16 mV).

In our experiments, we observe two opposite effects: (i) a stabilization of DPhPC membranes at low cholesterol amounts followed by (ii) a destabilization for cholesterol amounts higher than 5%. These tendencies are explained, as for the former experiments with bi-phospholipid systems, by a combination of different parameters that affect the molecular packing density.

The well-known function of cholesterol is to regulate the permeability and the properties of the membranes of mammalian cells [1,2]. This is achieved through various effects on the phospholipid molecules, ordering effects, condensing effects and the establishment of specific interactions with the phospholipids [1]. The presence of cholesterol subsequently results in (i) an increase in the order and the density of the phospholipid network [29,51], (ii) thickening of the membranes [52], and (iii) a reduction in the mobility of the phospholipid molecules [30,52]. These factors consequently disfavour the deformation of the bilayer and pore formation [24,33,52]. Interestingly, the effect of cholesterol depends on the structural properties of the phospholipids, and specifically occurs with saturated phospholipids [29,48] and lipids having a high melting temperature, T_m [53]. However, while DPhPC is saturated, it has a low T_m ($\leq 20°C$) [47] and it has been reported to have a similar effect on membranes as cholesterol [46]. As a consequence, DPhPC membranes are already densely packed and rigid. This density found in DPhPC membranes is accounted for by the formation of an intertwined network with neighbouring hydrocarbon chains being interdigitated [44,45]. Still, we assume that not all hydrocarbon chains are involved in this network and that there is some room for a few cholesterol molecules to insert into the membrane, bind to DPhPC molecules and condense the phospholipid network. This results in a further rigidification and stabilization of the membrane, and yields an increased resistance to the application of an electric field, as observed for cholesterol amounts up to 5% weight.

For higher cholesterol amounts, the membrane stability decreases. As already mentioned, there is little free space for cholesterol to insert into the dense network formed by DPhPC molecules, so further addition of cholesterol translates into the disentanglement of the hydrocarbon chains of DPhPC molecules and the subsequent rupture of the intertwined network. The membrane becomes less dense and cholesterol stops behaving as a condensing molecule but starts acting as a curvature-inducing molecule in the same manner as PE [21], further destabilizing the membrane. Consequently, above 5% cholesterol in the DPhPC membranes the progressive decrease of the electroporation threshold we measure is due to the rupture of the dense DPhPC network and the addition of a negative intrinsic monolayer curvature molecule, as observed for PE. Interestingly, the destabilizing effect of cholesterol is much higher than for PE. 20% weight of cholesterol in a DPhPC membrane leads to a V_{th} of 104 ± 52 mV against 160 ± 28 mV for 100% PE membranes. An explanation for this effect is that cholesterol is a rigid planar molecule, whereas PE is deformable. Cholesterol subsequently introduces larger defects in the mixed membrane and thereby facilitates pore formation upon application of an electric field.

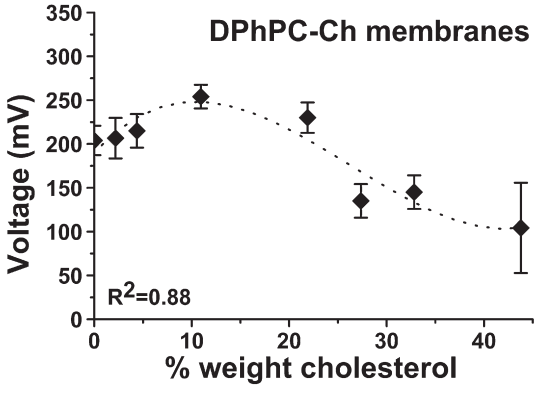

Fig. 3. Electroporation threshold V_{th} measured for DPhPC-Ch membranes. V_{th} is plotted against the weight percentage (0–20%) of cholesterol in the membrane. The dotted line represents the best fit for the data derived in Origin (OriginLab, Northampton, MA).

3.2. Proteins

In this section of this article, we consider the influence of another essential constituent of cellular membranes, proteins. We investigate not only the effect of the presence of proteins, but also that of the amount of proteins in a BLM.

We use a well-studied protein channel, α-hemolysin, that we can fairly easily incorporate in BLMs, as a model for membrane proteins. As its pore is always in the open state [54–56], the introduction of every pore generates a leakage pathway in the membrane and protein insertions can easily be identified by the apparition of characteristics jumps in the trans-membrane current. The insertion of every protein corresponds to a jump in the current of ~50 pA upon application of a DC voltage of 50 mV across the membrane as the channel has a 1 nS conductance.

3.2.1. Monitoring the protein density

Most experiments on proteins in BLMs focus on getting as few proteins as possible in these membranes enabling the study of individual proteins [57]. As we want to simulate real cell membrane conditions where proteins represent 50% of the weight of the membranes, experimentation with only a few proteins in the BLMs is not representative. Therefore, we adopt a more comprehensive approach and endeavour to monitor the amount of proteins we introduce in DPhPC membranes: from a single protein per membrane to a weight percentage of ~50%, to come as close as possible to a real-world situation. This differs from similar experiments found in the literature where small peptides (gramicidin A) that are able to form channels across the membrane are used, and the peptide is added in a known concentration to the lipid mixture before making the membranes [34]. We observe here the insertion of individual proteins in an already prepared DPhPC membrane.

The results of the experiments are summarized in Table 1. When the concentration of α-hemolysin in the reservoir is 2.5×10^{-2} μg/mL, we get dynamics of insertion of 1 protein every 10 minutes. This implies that if the buffer is refreshed after the first insertion, experiments at the single protein level are conceivable. When raising the α-hemolysin concentration in solution to 5 or 10×10^{-2} μg/mL, insertion proceeds

Table 1
Dynamics of insertion of α-hemolysin as a function of the protein concentration in solution: number of proteins inserted in the membrane every 10 min and corresponding protein densities (for a membrane with a given surface area of $\sim 9 \times 10^3$ μm^2).

Protein concentration in solution (μg/mL)	Dynamics of insertion (# proteins/10 min)[a]	Protein density ($\times 10^{-3}$ proteins/μm^2)[b]
2.5×10^{-2}	1	0.11
5×10^{-2}	3–10	0.33–1.1
10×10^{-2}	60–100	6.8–11

[a] Since one jump of ~50 pA corresponds to the insertion of one protein, the amount of proteins is determined using the total current increase.
[b] The protein density is calculated by dividing the total amount of proteins by the membrane surface area. The membrane surface area is calculated using equation 1 and an average measured capacitance of 40 ±11pF.

much faster, with typically 3–10 or 60–100 proteins per 10 min, respectively (see Fig. 4). Subsequently, by varying the protein concentration in solution and by refreshing the buffer solution after 10 minutes, we are able to modulate the protein density in the membrane from 0.11×10^{-3} (1 protein in the membrane) to 11×10^{-3} proteins/μm^2 (~100 proteins in the membrane) for membranes having an average surface area of $\sim9\times10^3$ μm^2. We will discuss these density values with respect to real-world situations in the discussion.

3.2.2. Phospholipid–protein interactions

Since we are able to monitor the protein insertion in BLMs we can characterize the membrane stability not only as a function of the presence of proteins but also as a function of their density in the membrane. Fig. 5 summarizes the results obtained for membranes containing various amounts of proteins. For a protein density below 5×10^{-3} proteins/μm^2 (<50 proteins in the membrane), V_{th} remains unchanged compared with mono-DPhPC membranes and is measured as 196 ± 22 mV. However, as soon as the protein density lies in a 5.5×10^{-3} to 14×10^{-3} proteins/μm^2 range (59–126 proteins per membrane), V_{th} becomes 226 ± 25 mV. Remarkably, for a protein density higher than 24×10^{-3} proteins/μm^2 (>212 proteins per membrane) V_{th} rises dramatically to above 800 mV, which corresponds to a 400% increase, and remains constant. These experiments exploring the effect of α-hemolysin on the membrane stability demonstrate that (i) the presence of proteins in the BLMs reduces the chance to create pores as indicated by the higher measured electroporation threshold V_{th}; and (ii) the higher the protein amount, the more stable the membrane. These observations are in good agreement with previous studies of Troiano et al. [34] on the effects of gramicidin D, a small pore-forming peptide, on the electroporation of lipid bilayers. They similarly report an increase in the electroporation threshold of 16% and 40% when gramicidin was added in a 1:500 and 1:15 peptide:phospholipid molar ratio, respectively. Furthermore, at a lower peptide concentration (1:10,000 molar ratio) the electroporation threshold remained unchanged. This also correlates with the findings of Navarrete and Santos-Sacchi [58] who suggest a change in the mechanical properties and the stiffness of the membrane in the presence of a protein, prestin. The experimental results of Troiano et al. have later been corroborated by molecular dynamics simulations, showing a significant reduction in pore formation in membranes containing gramicidin A peptides [35]. These simulations provide a model for the influence such a small peptide would have on a membrane and its properties. A two-fold effect is reported. Firstly, in close vicinity to the peptide (<2 nm), the membrane becomes thinner

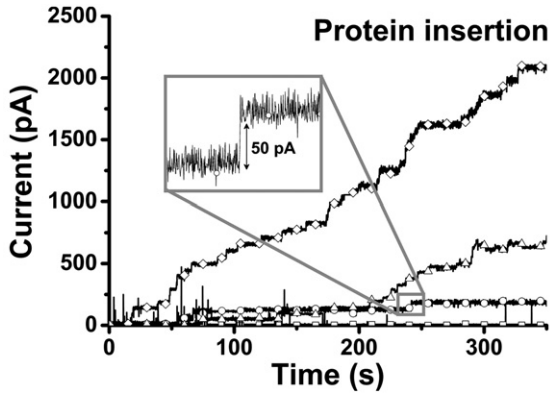

Fig. 4. Monitoring the insertion of α-hemolysin in DPhPC membranes. Leakage current measured across a DPhPC membrane as a function of the time upon application a 50 mV voltage. Protein concentrations of 2.5×10^{-3} μg/mL (*squares*), 5×10^{-3} μg/mL (*circles*), 10×10^{-3} μg/mL (*triangles*) and 25×10^{-3} μg/mL (*diamonds*). The jumps in the current correspond to the insertions of a single protein (see inset) as the insertion of one protein corresponds to an increase of 50 pA in the current (the conductance of a single α-hemolysin protein is 1 nS).

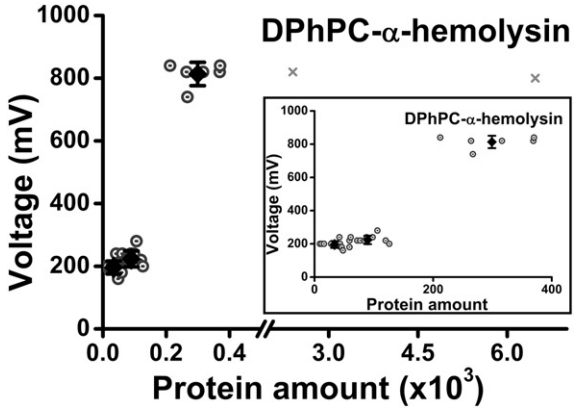

Fig. 5. Electroporation threshold V_{th} of α-hemolysin containing DPhPC membranes plotted against the amount of proteins introduced in the membrane. Inlay shows a zoom of the data for <400 proteins in the membrane. The gray circles represent individual measurements of V_{th} for a given protein concentration. The black diamonds represent the averaged V_{th} for an averaged amount of proteins. The gray crosses represent two measurements done with more than 360 proteins in the membrane (see Section 4.3 for more details).

to adapt to the height of the hydrophobic part of the peptide molecule while the packing density of the individual phospholipid molecules becomes loosened. Secondly, at longer distance (2–3 nm), an opposite process is observed: the phospholipid hydrocarbon chains become more ordered and the membrane thicker, lowering the probability for pore formation in the membrane. We expect similar phenomena to occur when replacing the small peptide gramicidin by a large protein channel such as α-hemolysin, but we assume that the radius and size of the two zones discussed above will be increased for a larger pore. According to the model proposed by Siu et al. [35], a 1:500 gramicidin: phospholipid ratio (see Troiano et al. [34]) translates in a 0.5% coverage of the membrane surface area by the proteins, while 2.5% of the membrane is affected by the presence of the peptides, resulting in a 16% increase in the measured electroporation threshold. In our experiments we see 13% and 400% increases in V_{th} for ~100 proteins and ~200 proteins, respectively, and this corresponds to molar ratios of $1{:}4.5\times10^8$ and $1{:}2.25\times10^8$, respectively. These data show that α-hemolysin has a longer distance effect than gramicidin or that another phenomenon must be taken into account to explain the influence of the protein on the membrane stability.

4. Discussion

We have studied the effect of three components found in natural cell membranes on the stability of planar mimics of membranes based on the DPhPC phospholipid: (i) the chemical and structural properties of various phospholipids, (ii) the effect of cholesterol and (iii) the influence of proteins (α-hemolysin). These three factors affect the stability of the membrane, and subsequently the probability to form pores in a membrane upon application of an electric field.

4.1. Lipidic contributions

Of the three constituents tested, the phospholipid composition has the lowest contribution on the membrane stability. However, we can still see clear trends in V_{th} variations related to the different chemical and structural phospholipid properties and particularly the subsequent packing density of the individual molecules. On one hand, the packing density of the phospholipids is increased when specific interactions are established between the molecules. This is illustrated with the condensing effect observed with cholesterol [50] but also to a less extent when electrostatic interactions take place between head groups of opposite charges (zwitterionic and negative). In both cases, the membrane becomes more stable and has a stronger resistance to

the application of an electric field. On the other hand, the packing density becomes loosened when unsaturated or non-zero intrinsic monolayer curvature phospholipids are used. The use of non-zero intrinsic monolayer curvature phospholipids results in bending of the membrane and the creation of packing defects while unsaturations tear phospholipid molecules apart.

While the mechanism of electropore formation is not yet fully elucidated, different models proposed from molecular dynamic simulation studies give insight into this process [12,13,36] and highlight how the packing density or pattern of the phospholipids affect the process of pore formation. As already mentioned in the introduction, pore formation proceeds in three steps, (i) a local enhancement of the electric field and the creation of water defects, (ii) the formation of a water file through the membrane and (iii) the rearrangement of the phospholipid molecules to create a hydrophilic pore [12], which are favoured or disfavoured depending on the phospholipid packing pattern, as explained below.

(i) *Local enhancement of the electric field and the creation of water defects*. This first step is favoured when packing defects are present in the membrane. DPhPC membranes are very stable and well-packed membranes [44–46]; there is little or no defect and little chance for insertion of water molecules. As a result, the probability for pore formation remains very low. The addition of non-zero intrinsic monolayer curvature phospholipids (PI, PE, PS) causes the amount of defects to increase [21], enabling local enhancement of the electric field and facilitating the insertion of water molecules. (ii) *Formation of a water file through the membrane, or creation of a hydrophilic pore*. Water molecules can move more easily into less densely packed membranes [12] to form a file through the membrane or a hydrophilic pore once a water defect is created. In case of DPhPC membranes, this step is again not likely as the creation of a water line requires the rupture of the intertwined network formed by the hydrocarbon chains. Similarly, if electrostatic interactions take place between phospholipid head groups (DPhPC/PI or DPhPC/PS) these interactions must be broken for water molecules to span the membrane. On the other hand, unsaturated phospholipids are less densely packed, giving space for water molecules to insert in the membrane and create a water file, increasing the likelihood of the second step of pore formation. (iii) *Rearrangement of the phospholipid molecules to create a hydrophobic pore*. The last step in the process of pore formation is the rearrangement of the phospholipid molecules to line the water file and create a hydrophilic pore. In general this last step is favoured with non-zero curvature lipids. The largest effect is still observed for lipids having a positive intrinsic monolayer curvature (PS, PI), those prefer to assemble as micellar structures and the edge of the pore resembles a semi-micelle (see Fig. 6A). In that case, a bulkier headgroup would result in a larger intrinsic monolayer curvature and a more marked stabilization effect. PI has a larger head group than PS, and thus a larger intrinsic monolayer curvature, so it will favour this step more than PS. Interestingly, lipids presenting a negative intrinsic monolayer curvature such as PE also contribute to pore stabilization but more for small pores: these lipids would line and circumvent the pore in the plane of the bilayer membrane [59], as represented in Fig. 6B. Again, the pore seen from the top resembles an inverted micelle, the preferred structure for those phospholipids. As the curvature of the pore in the plane of the membrane is larger for smaller pores, this stabilizing effect is more important for smaller pores than for larger ones for which the curvature will be negligible.

As a conclusion, all three steps are disfavoured in DPhPC membranes, and so is the creation of electropores. PE will favour the two first steps and the third step only in a pore-size dependent manner. Globally, its presence in the membrane has only a slight influence on the electroporation threshold (160 mV against 200 mV for DPhPC membranes). PI and PS favour all three steps, but the second step to a lesser extent as the presence of unsaturations is counterbalanced by the existence of electrostatic interactions between the head groups. Finally, as PI presents 4 unsaturations and a larger head group, its contribution to pore formation is higher. All together, the probability of pore formation would increase in the following order DPhPC<PE<PS<PI for the bi-phospholipidic systems we consider here, and this is in good agreement with our observations.

4.2. Cholesterol

Cholesterol gives an interesting and concentration-dependent two-fold effect in the 0–20% weight range. These results are nonetheless specific to our phospholipidic system as DPhPC forms an extremely dense and stable membrane, and they are expected to be different for other phospholipid species.

The natural role of cholesterol is to stiffen and order the membrane by strengthening the interactions between individual phospholipids forming the membrane [1,50]; this conformational order makes the membrane more resistant to external stress, increases its stability and lowers its permeability to water and ions. This is reflected by the higher amount of cholesterol present in the cytoplasmic membrane of cells (>30% mol) compared to those of intracellular organelles (<12% mol) [1,60]. In presence of cholesterol, the energetic cost to create water defects in natural membranes is dramatically increased, and cholesterol will prevent the creation of defects and water pores in the membrane [52]. In addition, the presence of cholesterol mostly

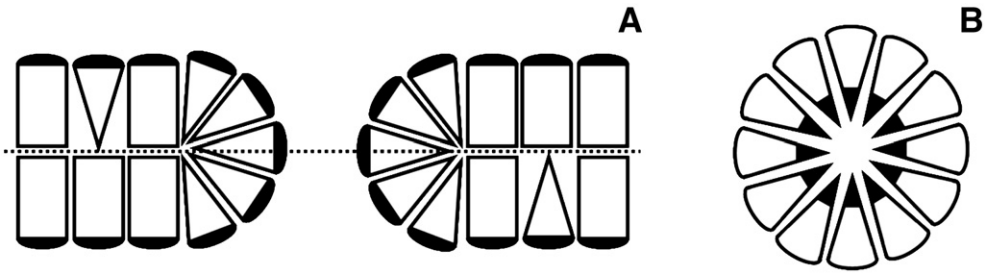

Fig. 6. Schematic showing of the effect of the intrinsic monolayer curvatures of the phospholipids on the last step of the pore formation process during electroporation; the lining of the pore by the phospholipid head groups. (A) Side view of a pore in a bilayer membrane containing zero and positive intrinsic monolayer curvature phospholipids. Phospholipids having a positive intrinsic monolayer curvature will prefer to line the edge of the pore along the normal of the bilayer as it resembles a semi-micellar structure. (B) Top view of a pore in the middle of the bilayer plane. The structure of the pore seen from the top resembles an inverted micelle; consequently, phospholipids having a negative intrinsic monolayer curvature prefer to surround the pore in the plane of the bilayer (indicated by the dotted line in (A)) and stabilize it.

induces thickening of the membrane, depending on the length of the phospholipid hydrocarbon chains [52].

However, we use DPhPC as basic units to prepare our membranes, and this belongs to the family of archaeal lipids [46,47]. This phospholipid is not found in natural membranes of mammalian cells but in those of archaebacteria that must resist harsh conditions such as high temperatures [47]. As a consequence, archaeal lipids must confer strong barrier properties and great stability to the membranes, as cholesterol would do for mammalian cell membranes. The effects of DPhPC are indeed similar to those of cholesterol [46]. DPhPC gives high molecular ordering of the membrane; it limits the trans-gauche conformation of the phospholipid molecules and their lateral and rotational motion while enhancing the motion of head groups (tilting). Finally, in both systems, a larger distance is found between head groups and subsequently, less head group interactions, either due to dominating cholesterol-phospholipid interactions or to the larger molecular area accounted by for the branched acyl chains [46].

It would be interesting to mix cholesterol to another phospholipid found in natural systems to be able to compare the results better to the outcome of mammalian cell electroporation experiments. In natural membranes, cholesterol is mainly present in stable microdomains found in the membrane, known as *lipid rafts* [61,62]. These domains are composed of a mixture of glycerolipids, sphingolipids and cholesterol. Therein, cholesterol prefers to bind to sphingolipids for shape reasons as sphingolipids are mostly saturated while glycerolipids present at least one unsaturation in natural systems. Future experiments with cholesterol should also take into account these microdomains, notably with the introduction of sphingolipids in our membranes and the study of ternary systems based on a mixture of glycero-, sphingolipids and cholesterol.

4.3. Proteins

Our double goal for the experiments with proteins was to be able to control their density in the membrane and to assess how the membrane stability would be affected by different amounts of proteins. For that purpose, our idea was to be able to cover a wide range of protein densities, from the single protein level up to a situation close to what is found in natural membranes, i.e. a 50% weight amount of proteins. To our best knowledge, no comparable study on the electrical stability of membranes depending on the concentration of channel proteins is reported in literature. Existing studies on the concentration dependency are limited to small peptides such a gramicidin A and D that can form transient pores, and these peptides were directly introduced in the lipid mixture in a known ratio, while we monitor their individual insertion in the membrane [34]. Navarette et al. studied the effect of the motor protein prestin found in the lateral plasma membrane of outer hair cells (OHCs) on the susceptibility to electroporation of these cells or transfected cells homogeneously expressing the protein. [58].

In this study we benefit from the fact that α-hemolysin is an open channel protein with a 1-nS conductance and the insertion of a single protein results in a leakage current. We use a 50 mV signal to make the insertion easy to detect from the noise of the signal, and every protein insertion gives rise to a 50-pA leakage current. The presence of 360 proteins in the membranes consequently leads to a leakage current of 18 nA which is the maximum current we can measure with our patch-clamp amplifier. As a consequence, in this configuration we are limited to a protein range of 1–360 proteins per membrane. To overcome this, the protein amount in the membrane can be measured afterwards using another method; employing the patch-clamp amplifier mode used to detect the formation of the GΩ seal during membrane preparation. This mode uses a low 1 mV voltage. Thereby, every protein gives rise to a leakage current of 1 pA allowing us to measure the presence of up to 18,000 proteins in the membrane. This was used for two experiments with ~2400 and ~6500 proteins, as shown in Fig. 5. Nonetheless, this method is more suitable for measuring large numbers of proteins afterwards and not to monitor the insertion of individual protein as the 1-pA leakage current given by a single protein may be difficult to distinguish from the signal noise.

The protein density is subsequently calculated from the total number of proteins inserted in the membrane and using the surface area of the membrane ($\sim 9\times10^3$ μm^2) assessed from a capacitance measurement (see Section 2.3). Until now we have achieved protein densities of up to 0.74 proteins/μm^2 (6500 proteins). For a comparison, a cell membrane contains a protein density of 1.25×10^5 proteins/μm^2 as 50% weight of proteins in a membrane corresponds to a ~40:1 molar ratio between phospholipids and proteins. As the molecular weights of DPhPC and α-hemolysin are 0.85 kDa and 33 kDa and a cell membrane contains approximately 5×10^6 phospholipids/μm^2 [2] a "natural" protein density in our model would be 1.25×10^5 proteins/μm^2. This is ~5–6 orders of magnitude higher than what we have achieved until now. An option to reach a higher protein density is to use smaller membranes. The advantage of using smaller membranes is that the smaller the membrane, the lower the noise level and the more sensitive the measurements, so that protein insertion could simply be followed by applying a 1 mV voltage. In that case, a "natural" protein density can be reached for instance by using a ~0.12 μm^2 membrane for 15,000 proteins inserted, which is achievable with a 0.5–1 μm diameter aperture.

The presence of α-hemolysin leads to a dramatic increase in V_{th} for more than 200 proteins in the membrane. Interestingly, there seems to be no apparent further variation in the V_{th} when the amount of proteins is further increased to ~6500 proteins. However, what precisely causes this stabilization of the membrane and why the threshold voltage reaches a plateau value is still not clear.

As mentioned, a similar stiffening and concentration-dependent effect is reported for both the small peptide gramicidin in a planar BLM model [34,35] and the motor protein prestin (~ 80 kDa) in a cell membrane environment [58]. This effect on the membrane stability is explained by a mechanical contribution in the case of prestin [58] and by local changes in the membrane properties and the ordering effect of the lipids in the case of gramicidin [34,35]. As the experiments performed with gramicidin are closer to our experimental system (BLMs and "controlled" concentration), we will focus on those for the rest of the discussion. Still, the effect of α-hemolysin on the bilayer stability is much larger than the effect of gramicidin, and this difference may have different reasons. Firstly, although the height of the trans-membrane part is similar for both α-hemolysin and gramicidin (~30 Å [56,63]), α-hemolysin is a much larger molecule with a molecular weight of 33 kDa and an outer stem diameter of 26 Å compared to a gramicidin dimer which has a molecular weight of 3.76 kDa and an outer diameter of 16 Å. In addition, α-hemolysin presents an extracellular cap of 100 Å diameter and 70 Å height [56] which may affect membrane stiffening. Therefore, the effect of the local changes in the membrane properties and the ordering effect of the lipids may be larger resulting in greater radii and sizes of the two zones, as described by Siu et al. [35]. This enlargement of the zones might also explain the plateau we observe in V_{th} for more than 200 proteins in the membranes; we can indeed hypothesize that the zones affected by the presence of the protein overlap from 200 proteins so that V_{th} does not increase any further. Secondly, while the pore of α-hemolysin is always in the open state, only part of the gramicidin units are involved in a pore structure as the latter is formed upon transient dimerization of two units. Thirdly, the presence of a pore gives rise to a leakage pathway in the membrane and in turn to a local decrease in the trans-membrane potential that disfavors pore formation. While this electrical contribution is reported to be negligible for gramicidin D [37], it could matter for α-hemolysin whose pore is larger (14–46 Å vs. 2 Å for gramicidin). As a conclusion,

when compared to gramicidin D, α-hemolysin may have a dual influence on the process of pore formation: a mechanical contribution as well as an electrical effect. We hypothesize that the mechanical stiffening of the membrane is greater in the case of α-hemolysin as a consequence of the higher molecular weight of the protein.

Future work will first aim at examining the plateau in the V_{th} above a certain concentration of molecules in the membrane to see if it is also present for other proteins or peptides. Following this, other proteins than gramicidin, prestin and α-hemolysin will be used to better understand the effect we observe for α-hemolysin. We particularly plan to use (i) proteins with various molecular weights and sizes to see how the structure size affects the process of pore formation, and (ii) proteins whose pore can be closed in order to decouple the mechanical and electrical contributions a pore protein such as α-hemolysin can have on membrane stability and on the process of pore formation.

Acknowledgements

The authors would like to thank the Physics of Fluids group from the University of Twente for their financial support and Martin Bennink and Yanina Cesa for their help and useful conversations.

References

[1] H. Ohvo-Rekila, B. Ramstedt, P. Leppimaki, J.P. Slotte, Cholesterol interactions with phospholipids in membranes, Prog. Lipid Res. 41 (2002) 66–97.
[2] B. Alberts, D. Bray, J. Lewis, M. Raff, K. Roberts, J.D. Watson, Molecular Biology of the Cell, 2 ed.Garland Publishing, Inc., New York, NY, USA, 1989.
[3] E. Neumann, M. Schaeferridder, Y. Wang, P.H. Hofschneider, Gene-transfer into mouse lyoma cells by electroporation in high electric-fields, EMBO J. 1 (1982) 841–845.
[4] E. Neumann, A.E. Sowers, C.A. Jordan (Eds.), Electroporation and Electrofusion in Cell Biology, Plenum Press, New York, USA, 1989.
[5] J.C. Weaver, Y.A. Chizmadzhev, Theory of electroporation: a review, Bioelectrochem. Bioenerget. 41 (1996) 135–160.
[6] D.C. Chang, B.M. Chassy, J.A. Saunders, A.E. Sowers (Eds.), Guide to Electroporation and Electrofusion, Academic Press, Inc., San Diego, CA, USA, 1992.
[7] C. Chen, S.W. Smye, M.P. Robinson, J.A. Evans, Membrane electroporation theories: a review, Med. Biol. Eng. Comput. 44 (2006) 5–14.
[8] M. Golzio, J. Teissie, M.P. Rols, Control by membrane order of voltage-induced permeabilization, loading and gene transfer in mammalian cells, Bioelectrochemistry 53 (2001) 25–34.
[9] C. Chen, J.A. Evans, M.P. Robinson, S.W. Smye, P. O'Toole, Measurement of the efficiency of cell membrane electroporation using pulsed ac fields, Phys. Med. Biol. 53 (2008) 4747–4757.
[10] L.V. Chernomordik, S.I. Sukharev, S.V. Popov, V.F. Pastushenko, A.V. Sokirko, I.G. Abidor, Y.A. Chizmadzhev, The electrical breakdown of cell and lipid-membranes—the similarity of phenomenologies, Biochim. Biophys. Acta 902 (1987) 360–373.
[11] S.J. Marrink, A.H. de Vries, D.P. Tieleman, Lipids on the move: Simulations of membrane pores, domains, stalks and curves, Biochim. Biophys. Acta 1788 (2009) 149–168.
[12] D.P. Tieleman, The molecular basis of electroporation, Biophys. J. 86 (2004) 371a–372a.
[13] R.A. Bockmann, B.L. de Groot, S. Kakorin, E. Neumann, H. Grubmuller, Kinetics, statistics, and energetics of lipid membrane electroporation studied by molecular dynamics simulations, Biophys. J. 95 (2008) 1837–1850.
[14] M. Hibino, H. Itoh, K. Kinosita, Time courses of cell electroporation as revealed by submicrosecond imaging of transmembrane potential, Biophys. J. 64 (1993) 1789–1800.
[15] W. Krassowska, P.D. Filev, Modeling electroporation in a single cell, Biophys. J. 92 (2007) 404–417.
[16] S. Koronkiewicz, S. Kalinowski, K. Bryl, Programmable chronopotentiometry as a tool for the study of electroporation and resealing of pores in bilayer lipid membranes, Biochim. Biophys. Acta 1561 (2002) 222–229.
[17] K.C. Melikov, V.A. Frolov, A. Shcherbakov, A.V. Samsonov, Y.A. Chizmadzhev, L.V. Chernomordik, Voltage-induced nonconductive pre-pores and metastable single pores in unmodified planar lipid bilayer, Biophys. J. 80 (2001) 1829–1836.
[18] J.C. Weaver, Electroporation of biological membranes from multicellular to nano scales, IEEE Trans. Dielect. Eelectr. In (10) (2003) 754–768.
[19] A. Diederich, G. Bahr, M. Winterhalter, Influence of surface charges on the rupture of black lipid membranes, Physical Rev. E 58 (1998) 4883–4889.
[20] M.J. Ziegler, P.T. Vernier, Interface water dynamics and porating electric fields for phospholipid bilayers, J. Phys. Chem. B 112 (2008) 13588–13596.
[21] S.W. Hui, A. Sen, Effects of lipid packing on polymorphic phase-behavior and membrane-properties, Proc. Natl. Acad. Sci. U. S. A. 86 (1989) 5825–5829.
[22] L.V. Chernomordik, M.M. Kozlov, G.B. Melikyan, I.G. Abidor, V.S. Markin, Y.A. Chizmadzhev, The shape of lipid molecules and monolayer membrane-fusion, Biochim. Biophys. Acta 812 (1985) 643–655.
[23] S. Kakorin, U. Brinkmann, E. Neumann, Cholesterol reduces membrane electroporation and electric deformation of small bilayer vesicles, Biophys. Chem. 117 (2005) 155–171.
[24] S. Koronkiewicz, S. Kalinowski, Influence of cholesterol on electroporation of bilayer lipid membranes: chronopotentiometric studies, Biochim. Biophys. Acta 1661 (2004) 196–203.
[25] M. Kotulska, S. Koronkiewicz, S. Kalinowski, Cholesterol induced changes in the characteristics of the time series from planar lipid bilayer membrane during electroporation, Acta Phys. Pol. B 33 (2002) 1115–1129.
[26] D. Needham, R.M. Hochmuth, Electro-mechanical permeabilization of lipid vesicles—role of membrane tension and compressibility, Biophys. J. 55 (1989) 1001–1009.
[27] P. Shil, S. Bidaye, P.B. Vidyasagar, Analysing the effects of surface distribution of pores in cell electroporation for a cell membrane containing cholesterol, J. Phys. D: Appl. Phys. (2008) 41.
[28] B. Dekruijff, P.R. Cullis, G.K. Radda, Outside–inside distributions and sizes of mixed phosphatidylcholine-cholesterol vesicles, Biochim. Biophys. Acta 436 (1976) 729–740.
[29] J.N. Israelachvili, D.J. Mitchell, Model for packing of lipids in bilayer membranes, Biochim. Biophys. Acta 389 (1975) 13–19.
[30] E. Karatekin, O. Sandre, H. Guitouni, N. Borghi, P.H. Puech, F. Brochard-Wyart, Cascades of transient pores in giant vesicles: line tension and transport, Biophys. J. 84 (2003) 1734–1749.
[31] Z. Chen, R.P. Rand, The influence of cholesterol on phospholipid membrane curvature and bending elasticity, Biophys. J. 73 (1997) 267–276.
[32] C.J. Dekker, W.S.M.G. Vankessel, J.P.G. Klomp, J. Pieters, B. Dekruijff, Synthesis and polymorphic phase-behavior of poly-unsaturated phosphatidylcholines and phosphatidylethanolamines, Chem. Phys. Lipids 33 (1983) 93–106.
[33] S. Raffy, J. Teissie, Control of lipid membrane stability by cholesterol content, Biophys. J. 76 (1999) 2072–2080.
[34] G.C. Troiano, K.J. Stebe, R.M. Raphael, L. Tung, The effects of gramicidin on electroporation of lipid bilayers, Biophys. J. 76 (1999) 3150–3157.
[35] S.W.I. Siu, R.A. Bockmann, Electric field effects on membranes: gramicidin A as a test ground, J. Struct. Biol. 157 (2007) 545–556.
[36] M. Tarek, Membrane electroporation: a molecular dynamics simulation, Biophys. J. 88 (2005) 4045–4053.
[37] G.C. Troiano, L. Tung, V. Sharma, K.J. Stebe, The reduction in electroporation voltages by the addition of a surfactant to planar lipid bilayers, Biophys. J. 75 (1998) 880–888.
[38] D. Moldovan, D. Pinisetty, R.V. Devireddy, Molecular dynamics simulation of pore growth in lipid bilayer membranes in the presence of edge-active agents, Appl. Phys. Lett. (2007) 91.
[39] S.N. Murthy, A. Sen, S.W. Hui, Surfactant-enhanced transdermal delivery by electroporation, J. Controlled Release 98 (2004) 307–315.
[40] L. Tung, G.C. Troiano, V. Sharma, R.M. Raphael, K.J. Stebe, Changes in electroporation thresholds of lipid membranes by surfactants and peptides, Ann. N. Y. Acad. Sci. 888 (1999) 249-265.
[41] P. Mueller, W.C. Wescott, D.O. Rudin, H.T. Tien, Methods for formation of single bimolecular lipid membranes in aqueous solution, J. Phys. Chem. 67 (1963) 534–535.
[42] A. Wiese, U. Seydel, Bacterial toxins: methods and protocols, in: O. Holst (Ed.), Methods Mol. Biol. Humana Press Inc., Totowa, NJ, 2000, pp. 355–370.
[43] D.P. Nikolelis, U.J. Krull, A.L. Ottova, H.T. Tien, Bilayer lipid membranes and other lipid-based methods, in: R. Taylor, J. Schultz (Eds.), Handbook of Chemical and Biological Sensors, Institute of Physics Publishing, Bristol, UK, 1996, pp. 221–256.
[44] T. Husslein, D.M. Newns, P.C. Pattnaik, Q.F. Zhong, P.B. Moore, M.L. Klein, Constant pressure and temperature molecular-dynamics simulation of the hydrated diphytanolphosphatidylcholine lipid bilayer, J. Chem. Phys. 109 (1998) 2826–2832.
[45] W. Shinoda, M. Mikami, T. Baba, M. Hato, Molecular dynamics study on the effect of chain branching on the physical properties of lipid bilayers: structural stability, J. Phys. Chem. B 107 (2003) 14030–14035.
[46] W. Shinoda, M. Mikami, T. Baba, M. Hato, Dynamics of a highly branched lipid bilayer: a molecular dynamics study, Chem. Phys. Lett. 390 (2004) 35–40.
[47] T. Kitano, T. Onoue, K. Yamauchi, Archaeal lipids forming a low energy-surface on air–water interface, Chem. Phys. Lipids 126 (2003) 225–232.
[48] P.R. Cullis, B. Dekruijff, Lipid polymorphism and the functional roles of lipids in biological-membranes, Biochim Biophys. Acta 559 (1979) 399–420.
[49] D. Papahadjopoulos, N. Miller, Phospholipid model membranes. I. Structural characteristics of hydrated liquid crystals, Biochim. Biophys. Acta 135 (1967) 624–638.
[50] T. Rog, M. Pasenkiewicz-Gierula, I. Vattulainen, M. Karttunen, Ordering effects of cholesterol and its analogues, Biochim. Biophys. Acta 1788 (2009) 97–121.
[51] R.A. Demel, Vandeene Ll, B.A. Pethica, Monolayer interactions of phospholipids and cholesterol, Biochim. Biophys. Acta 135 (1967) 11–19.
[52] W.F.D. Bennett, J.L. MacCallum, D.P. Tieleman, Thermodynamic analysis of the effect of cholesterol on dipalmitoylphosphatidylcholine lipid membranes, J. Am. Chem. Soc. 131 (2009) 1972–1978.
[53] S.L. Keller, A. Radhakrishnan, H.M. McConnell, Saturated phospholipids with high melting temperatures form complexes with cholesterol in monolayers, J. Phys. Chem. B 104 (2000) 7522–7527.
[54] S. Bhakdi, J. Tranumjensen, Alpha-toxin of *Staphylococcus aureus*, Microbiol. Rev. 55 (1991) 733–751.
[55] E. Gouaux, Alpha-hemolysin from *Staphylococcus aureus*: an archetype of beta-barrel, channel-forming toxins, J. Struct. Biol. 121 (1998) 110–122.

[56] L.Z. Song, M.R. Hobaugh, C. Shustak, S. Cheley, H. Bayley, J.E. Gouaux, Structure of staphylococcal alpha-hemolysin, a heptameric transmembrane pore, Science 274 (1996) 1859–1866.
[57] H. Suzuki, S. Takeuchi, Microtechnologies for membrane protein studies, Anal. Bioanal. Chem. 391 (2008) 2695–2702.
[58] E.G. Navarrete, J. Santos-Sacchi, On the effect of prestin on the electrical breakdown of cell membranes, Biophys. J. 90 (2006) 967–974.
[59] R.M. Epand, Lipid polymorphism and protein–lipid interactions, Biochim. Biophys. Acta-Rev. Biomembr. 1376 (1998) 353–368.
[60] P.L. Yeagle, Cholesterol and the cell-membrane, Biochim. Biophys. Acta 822 (1985) 267–287.
[61] D.A. Brown, E. London, Structure of detergent-resistant membrane domains: Does phase separation occur in biological membranes? Biochem. Biophys. Res. Commun. 240 (1997) 1–7.
[62] D.A. Brown, E. London, Structure and function of sphingolipid- and cholesterol-rich membrane rafts, J. Biol. Chem. 275 (2000) 17221–17224.
[63] B.A. Wallace, Recent advances in the high resolution structures of bacterial channels: Gramicidin A, J. Struct. Biol. 121 (1998) 123–141.